Neumann Expansion for Stochastic Finite Element Analysis

By Fumio Yamazaki,[1] Associate Member, ASCE, Masanobu Shinozuka,[2] Member, ASCE, and Gautam Dasgupta,[3] Member, ASCE

Abstract: With the aid of the finite element method, the present paper deals with the problem of structural response variability resulting from the spatial variability of material properties of structures, when they are subjected to static loads of a deterministic nature. The spatial variabilities are modeled as two-dimensional stochastic fields. The finite element discretization is performed in such a way that the size of each element is sufficiently small. Then, the present paper takes advantage of the Neumann expansion technique in deriving the finite element solution for the response variability within the framework of the Monte Carlo method. The Neumann expansion technique permits more detailed comparison between the perturbation and Monte Carlo solutions for accuracy, convergence, and computational efficiency. The result from such a Monte Carlo method is also compared with that based on the commonly used perturbation method. The comparison shows that the validity of the perturbation method is limited to the cases where the material property variation has a relatively small coefficient of variation, particularly when Young's modulus itself is assumed to form a stochastic field.

Introduction

Most modern structural systems possess high degrees of structural complexity. Therefore, when their structural behavior is to be predicted under various loading and environmental conditions, advanced analytical and numerical techniques, notably the finite element method, are required and are indeed extensively used in various fields of structural engineering. However, most of these applications are limited to dealing with deterministic loading and environmental conditions despite the fact that they intrinsically involve randomness and uncertainty to a considerable degree.

With the aid of the finite element method, the present paper deals with the problem of structural response variability resulting from the spatial variability of the material properties of structures when they are subjected to static loads of a deterministic nature. The problem of response variability when structures with spatially stochastic material properties are subjected to random forces will be examined in the future as a sequel to the present work.

The spatial variabilities are modeled as a multivariate stochastic field. Its

[1]Res. Engr., Ohsaki Res. Inst., Shimizu Constr. Co., Ltd., Tokyo, Japan; formerly, Visiting Scholar, Columbia Univ., New York, NY 10027.

[2]Renwick Prof. of Civ. Engrg., Dept. of Civ. Engrg. and Engrg. Mech., Columbia Univ., New York, NY 10027.

[3]Assoc. Prof., Dept. of Civ. Engrg. and Engrg. Mech., Columbia Univ., New York, NY 10027.

Note. Discussion open until January 1, 1989. To extend the closing date one month, a written request must be filed with the ASCE Manager of Journals. The manuscript for this paper was submitted for review and possible publication on October 27, 1986. This paper is part of the *Journal of Engineering Mechanics*, Vol. 114, No. 8, August, 1988. ©ASCE, ISSN 0733-9399/88/0008-1335/$1.00 + $.15 per page. Paper No. 22674.

component fields are possibly correlated. In this respect, it is noted that the analysis of multidimensional and multivariate stochastic fields, particularly in conjunction with the digital generation of their sample functions, was carried out earlier by Shinozuka (1972a, 1972b, 1974; Shinozuka and Jan 1972). A number of papers demonstrating the applications of stochastic field theory in structural engineering and engineering mechanics were published by Shinozuka and his associates [e.g., Astill et al. (1972), Iyengar and Shinozuka (1972), Shinozuka and Astill (1972), Shinozuka and Wen (1972), Shinozuka et al. (1976, 1977), and Vaicaitis et al. (1972, 1973)]. In this respect, a recent book by Vanmarcke (1983) is also noted.

The finite element discretization may be performed in such a way that the size of each element (of appropriate dimensionality) is sufficiently small. In fact to be conservative, under the assumption of homogeneity of the stochastic field representing the material property variability, the size must be small in comparison with the wave length of the harmonic component having the largest wave number indicated by a spectral density function that describes the field, if such a component can be identified. If not, whether or not the size is small enough ought to be examined in comparison with the "scale of correlation" associated with the stochastic field under study (Harada and Shinozuka 1986b). This issue will be addressed again later in this paper. It is obvious, however, that the question of size must also be addressed from the stress or strain gradient point of view; a finer discretization is needed in a location where the gradient is more significant. Thus, when we have structural materials whose properties vary spatially, the size of the discretization must satisfy the requirements from the stress gradient as well as material property variability points of view. The issue is actually related to the problem arising from the fact that the finite element method approximates the solution by virtue of assumed shape functions that are not necessarily, and in fact most probably are not, consistent with the spatial variabilities of the material properties of the structures. This issue is not easily resolved. In the meantime, however, it is suggested that the size of discretization be made small enough so that the material properties may be assumed to be constant within each element. The constancy of the material property values, at least within each element, is an assumption consistent with the way in which standard finite element analyses are performed.

Finite element solutions for response variability can be obtained in approximation by means of perturbation and related methods [e.g., Baecher and Ingra (1981), Der Kiureghian (1985), Cambou (1975), Handa and Andersson (1981), Hisada and Nakagiri (1981, 1985), and Vanmarcke and Grigoriu (1983)]. In particular, first-order perturbation solutions appear to be reasonably accurate for small material property variability. However, perturbation methods usually suffer from questions on their accuracy, convergence, and computational efficiency. These questions become more crucial as higher order solutions are sought, as the degree of the material property variability becomes more pronounced, and when dynamic, particularly transient and wave propagation, problems must be considered.

The present paper takes advantage of the Neumann expansion technique in deriving the finite element solution for the response variability within the framework of Monte Carlo methods. The Neumann expansion technique

permits more detailed comparison between the perturbation and Monte Carlo solutions for accuracy, convergence, and computational efficiency.

Spatial Variations of Material Properties

Analytical Modeling of Stochastic Fields

The spatial variation of material properties, such as Young's modulus or Poisson's ratio, is assumed to be a two-dimensional homogeneous stochastic process in this study. The fluctuating component $a(\mathbf{x})$ of a material property is then assumed to have mean zero

$$E[a(\mathbf{x})] = 0 \quad \ldots\ldots (1)$$

and auto-correlation function

$$R_{aa}(\boldsymbol{\xi}) = E[a(\mathbf{x})a(\mathbf{x}+\boldsymbol{\xi})] \quad \ldots\ldots (2)$$

where $\mathbf{x} = [x\ y]^T$ indicates the position vector; and $\boldsymbol{\xi} = [\xi_x\ \xi_y]^T$, the separation vector between two points $\mathbf{x}$ and $\mathbf{x} + \boldsymbol{\xi}$.

If the randomness of the spatial variation is isotropic, the autocorrelation function of the spatial variation is supposed to be a function only of the distance $|\boldsymbol{\xi}|$. While the analysis procedure used in the present paper does not require this assumption, the following form of an isotropic autocorrelation function is considered for the present analysis:

$$R_{aa}(\boldsymbol{\xi}) = \sigma_0^2 \exp\left[-\left(\frac{|\boldsymbol{\xi}|}{d}\right)^2\right] \quad \ldots\ldots (3)$$

in which d = a positive parameter such that the larger it is, the more slowly the correlation disappears. In fact, for this autocorrelation function, d can be defined as the scale of correlation (Harada and Shinozuka 1986a; Lumley 1970; Monin and Yaglom 1971; Tatarski 1961), and σ_0 = the standard deviation of the stochastic field. With the aid of the Wiener-Khintchine relationship, the spectral density function corresponding to the assumed autocorrelation function is given by

$$S_{aa}(\boldsymbol{\kappa}) = \sigma_0^2 \frac{d^2}{4\pi} \exp\left[-\left(\frac{d|\boldsymbol{\kappa}|}{2}\right)^2\right] \quad \ldots\ldots (4)$$

in which $\boldsymbol{\kappa} = [\kappa_x\ \kappa_y]^T$ = the wave number vector. This pair of autocorrelation and spectral density functions are used in this study for numerical examples.

When the finite element method is used, the structure is divided into an appropriate number of finite elements of small size. As mentioned earlier, the size of each finite element must be small enough from the material property variability, as well as the stress gradient, points of view. From the former point of view, it must be small enough so that the property values can be considered approximately constant within each element. Thus, if there are n finite elements in total, then there are n material property values associated with these n elements. Consider only the fluctuating components of the homogeneous stochastic field, which is assumed to model the material property variation around its expected value. Then these n values, $a_i = a(\mathbf{x}_i)$ $(i = 1, 2, \ldots, n)$, are random with mean zero but

correlated, where $\mathbf{x}_i$ = the location of the centroid of element i. Their correlational characteristics can be specified in terms of the covariance matrix $\mathbf{C}_{aa}$, whose ij-component is given by

$$c_{ij} = \text{Cov}\,[a_i a_j] = E[a_i a_j] = R_{aa}(\xi_{ij}) \quad (5)$$

where $\xi_{ij} = \mathbf{x}_j - \mathbf{x}_i$ = the separation between the centroids of elements i and j.

A vector $\mathbf{a} = [a_1\ a_2\ \ldots\ a_n]^T$ can then be generated by

$$\mathbf{a} = \mathbf{LZ} \quad (6)$$

in which $\mathbf{Z} = [Z_1 Z_2\ \ldots\ Z_n]^T$ = a vector consisting of n independent Gaussian random variables with mean zero and unit standard deviation; and $\mathbf{L}$ = a lower triangular matrix obtained by the Cholesky decomposition of the covariance matrix $\mathbf{C}_{aa}$. Thus

$$E[\mathbf{ZZ}^T] = \mathbf{I} \quad (7a)$$

$$\mathbf{LL}^T = \mathbf{C}_{aa} \quad (7b)$$

where $\mathbf{I}$ = the identity matrix of appropriate dimensions. The vector $\mathbf{a}$ generated by using Eq. 6 satisfies the original covariance matrix:

$$E[\mathbf{aa}^T] = E[\mathbf{LZ}(\mathbf{LZ})^T] = \mathbf{L}E[\mathbf{ZZ}^T]\mathbf{L}^T = \mathbf{C}_{aa} \quad (8)$$

Once the Cholesky decomposition is accomplished, different sample vectors of $\mathbf{a}$ are easily obtained with the aid of Eq. 6 by generating different samples for the independent Gaussian random vectors $\mathbf{Z}$. Thus, for the type of problem we are interested in here, this technique can be conveniently used for Monte Carlo simulation, although other methods such as spectral decomposition of the covariance matrix, the spectral representation technique (Shinozuka 1972a, 1972b, 1974, 1985; Shinozuka and Jan 1972), and the ARMA technique can also be used. It is cautioned that the Cholesky decomposition may become "numerically" difficult if the as are highly correlated with each other; in which case, however, these other methods, particularly the method of spectral decomposition of the covariance matrix, can be used.

Finite Element Analysis

The standard finite element analysis method for linear static problems is briefly described in order to facilitate the introduction of the following sections. Assuming an appropriate shape function $\mathbf{N}$, the displacement $\mathbf{u}^{(e)}$ within element e is represented by

$$\mathbf{u}^{(e)} = \mathbf{N}\mathbf{u}_e \quad (9)$$

where $\mathbf{u}_e$ = the nodal displacement vector of element e. By differentiating Eq. 9, the strain $\boldsymbol{\varepsilon}_e$ within element e can be obtained as

$$\boldsymbol{\varepsilon}_e = \mathbf{B}_e \mathbf{u}_e \quad (10)$$

in which $\mathbf{B}_e$ = the matrix determined from the shape function and geometric condition of the element. The stress $\boldsymbol{\sigma}_e$ within element e is also given by

$$\boldsymbol{\sigma}_e = \mathbf{D}_e \boldsymbol{\varepsilon}_e \quad (11)$$

in which $\mathbf{D}_e$ = the elasticity matrix. The element stiffness matrix $\mathbf{k}_e$ can be obtained by applying the virtual work principal over the volume of the element

$$\mathbf{k}_e = \int_{vol.} \mathbf{B}_e^T \mathbf{D}_e \mathbf{B}_e \, dV \quad (12)$$

The global stiffness matrix $\mathbf{K}$ is obtained by assembling the element stiffness matrices over the entire region. Then, applying boundary conditions, the equilibrium equation to solve is written as

$$\mathbf{KU} = \mathbf{F} \quad (13)$$

in which $\mathbf{U}$ = the unknown displacement vector; and $\mathbf{F}$ = the external force vector.

In the present study, a two-dimensional plane stress problem is considered as an example. In this case, $\mathbf{D}_e$ is known as

$$\mathbf{D}_e = \frac{E_e}{1-\nu_e^2}\begin{bmatrix} 1 & \nu_e & 0 \\ & 1 & 0 \\ \text{sym.} & & \dfrac{1-\nu_e}{2} \end{bmatrix} \quad (14)$$

in which E_e = Young's modulus; and ν_e = Poisson's ratio of element e. A rectangular element with four nodes is used here. The integration in Eq. 12 is performed in "closed form" with the aid of the symbolic manipulation program SMP (Inference Corp. 1983).

Neumann Expansion Method

The equilibrium equation formulated by the finite element method can obviously be solved by taking the inverse of the stiffness matrix as

$$\mathbf{U} = \mathbf{K}^{-1}\mathbf{F} \quad (15)$$

However, it is well-known that matrix inversions require a large amount of CPU time. Also, $\mathbf{K}^{-1}$ is no longer banded, although $\mathbf{K}$ is usually narrowly banded. Thus, the multiplication on the right-hand side of Eq. 15 cannot be performed efficiently if the number of degrees-of-freedom is large.

An alternative way to directly solve Eq. 13 is to first take the Cholesky decomposition of $\mathbf{K}$ and to obtain the lower triangular matrix $\mathbf{L}$ as

$$\mathbf{LL}^T = \mathbf{K} \quad (16)$$

and then to solve the following equation with respect to the unknowns $\mathbf{X}$ and $\mathbf{U}$ in turn:

$$\mathbf{LX} = \mathbf{F} \quad (17a)$$

$$\mathbf{L}^T\mathbf{U} = \mathbf{X} \quad (17b)$$

It is important to note that, since the lower triangular matrix $\mathbf{L}$ preserves the same bandwidth as $\mathbf{K}$, $\mathbf{X}$ and $\mathbf{U}$ can be solved from Eq. 17 efficiently.

Under the assumption that $\mathbf{K}$ contains parameters that are subjected to spatial variabilities, decompose $\mathbf{K}$ into two matrices:

$$\mathbf{K} = \mathbf{K}_0 + \Delta\mathbf{K} \quad (18)$$

where $\mathbf{K}_0$ = the stiffness matrix in which the spatially variable parameters are replaced by their representative values (mean values or medians in this study); and $\Delta\mathbf{K}$ consists of components representing the "deviatoric parts" of the corresponding components in $\mathbf{K}$: $\Delta\mathbf{K} = \mathbf{K} - \mathbf{K}_0$. The solution $\mathbf{U}_0$ which corresponds to $\mathbf{K}_0$ can be obtained as

$$\mathbf{K}_0\mathbf{U}_0 = \mathbf{F} \quad (19a)$$

$$\mathbf{U}_0 = \mathbf{K}_0^{-1}\mathbf{F} \quad (19b)$$

The Neumann expansion of $\mathbf{K}^{-1}$ takes the following form with $\mathbf{P} = \mathbf{K}_0^{-1}\Delta\mathbf{K}$:

$$\mathbf{K}^{-1} = (\mathbf{K}_0 + \Delta\mathbf{K})^{-1} = (\mathbf{I} - \mathbf{P} + \mathbf{P}^2 - \mathbf{P}^3 + \cdots)\mathbf{K}_0^{-1} \quad (20)$$

Introducing Eq. 20 into Eq. 15 and using Eq. 19, the solution vector $\mathbf{U}$ is represented by the following series as

$$\mathbf{U} = \mathbf{U}_0 - \mathbf{P}\mathbf{U}_0 + \mathbf{P}^2\mathbf{U}_0 - \mathbf{P}^3\mathbf{U}_0 + \cdots \quad (21a)$$

$$\mathbf{U} = \mathbf{U}_0 - \mathbf{U}_1 + \mathbf{U}_2 - \mathbf{U}_3 + \cdots \quad (21b)$$

This series solution is equivalent to the following recursive equation:

$$\mathbf{K}_0\mathbf{U}_i = \Delta\mathbf{K}\mathbf{U}_{i-1}, \qquad i = 1, 2, \ldots \quad (22)$$

Thus, once the Cholesky decomposition of $\mathbf{K}_0$ is obtained as $\mathbf{L}_0\mathbf{L}_0^T = \mathbf{K}_0$, and $\mathbf{U}_0$ is obtained using the algorithm represented by Eq. 17, then the same algorithm can be used to obtain $\mathbf{U}_i$ iteratively with the aid of Eq. 22. The expansion series in Eq. 21 may be terminated after a few terms if convergence of the series is confirmed by using the following criterion:

$$\frac{\|\mathbf{U}_i\|_2}{\left\|\sum_{k=0}^{i}(-1)^k\mathbf{U}_k\right\|_2} \leqq \delta_{\text{err}} \quad (23)$$

where δ_{err} = the allowable error to be specified for convergence (δ_{err} = 0.01 is used for the numerical examples in this paper), and $\|\cdot\|_2$ = the vector norm (length) defined by

$$\|\mathbf{U}\|_2 = \sqrt{\mathbf{U}^T\mathbf{U}} \quad (24)$$

The most outstanding feature of this approach in the case of Monte Carlo simulation for the spatial variation of material properties is that matrix factorization is required only once for all samples, and the rest of the computational process can fully utilize the banded characteristics of $\Delta\mathbf{K}$ and $\mathbf{L}_0$. Therefore, the computational time and costs may be reduced considerably.

It is well-known that the Neumann expansion shown in Eq. 20 converges if the absolute values of all the eigenvalues of $\mathbf{P} = \mathbf{K}_0^{-1}\Delta\mathbf{K}$ are less than 1.

However, this convergence criterion can be easily met irrespective of how large each component of the deviation matrix $\Delta\mathbf{K}$ is in comparison with the corresponding component of $\mathbf{K}$. This can be done by choosing, for each sample, a reference matrix $\mathbf{K}_0^*$ for expansion in such a way that

$$\mathbf{K} = \mathbf{K}_0^* + \Delta\mathbf{K}^* \quad (25a)$$

$$\mathbf{K}_0^* = m\mathbf{K}_0 \quad (25b)$$

where m = a scalar that is chosen to satisfy the convergence criterion of the sample. Then, Eqs. 21 and 22 must be modified into the following form:

$$\mathbf{U} = \mathbf{U}_0^* - \mathbf{U}_1^* + \mathbf{U}_2^* - \mathbf{U}_3^* + \cdots \quad (26)$$

$$\mathbf{K}_0^*\mathbf{U}_i^* = \Delta\mathbf{K}^*\mathbf{U}_{i-1}^*, \qquad (i = 1, 2, \ldots) \quad (27)$$

However, this change in the reference matrix from $\mathbf{K}_0$ to $\mathbf{K}_0^*$ induces almost no additional computational effort to derive the solution because of the following relationships:

$$\mathbf{U}_0^* = \frac{1}{m}\mathbf{U}_0 \quad (28)$$

$$\mathbf{K}_0\mathbf{U}_i^* = \frac{1}{m}\Delta\mathbf{K}^*\mathbf{U}_{i-1}^* = \left(\frac{1}{m}\mathbf{K} - \mathbf{K}_0\right)\mathbf{U}_{i-1}^* \quad (29)$$

Thus, by replacing $\mathbf{U}_0$ and $\Delta\mathbf{K}$ with $\mathbf{U}_0/m$ and $(\mathbf{K}/m - \mathbf{K}_0)$, respectively, the same decomposition algorithm involving $\mathbf{L}_0$ as used in Eq. 22 can be applied to Eq. 27 for iterative solutions.

The possible range of m is determined by eigenvalue analysis. Assuming that Φ_k is the kth eigenvector, and λ_k is the kth eigenvalue of $\mathbf{P}$, so that $|\lambda_1| \geqq |\lambda_2| \geqq \ldots \geqq |\lambda_n|$, the following equation is obtained:

$$(\mathbf{K}_0^{-1}\Delta\mathbf{K})\Phi_k = \lambda_k\Phi_k, \qquad (k = 1, 2, \ldots, n) \quad (30)$$

If λs are such that $|\lambda_k| \geqq 1$, the reference matrix of expansion must be changed from $\mathbf{K}_0$ to $\mathbf{K}_0^*$ in order to make the expansion convergent. Then, the deviatoric part of $\mathbf{K}$ is written as

$$\Delta\mathbf{K}^* = \mathbf{K} - \mathbf{K}_0^* = (1 - m)\mathbf{K}_0 + \Delta\mathbf{K} \quad (31)$$

The eigenvalue and eigenvector of the product, $(\mathbf{K}_0^*)^{-1}\Delta\mathbf{K}^*$, are also represented by an equation similar to Eq. 30 as

$$[(\mathbf{K}_0^*)^{-1}\Delta\mathbf{K}^*]\Phi_{k'}^* = \lambda_{k'}^*\Phi_{k'}^*, \qquad (k' = 1, 2, \ldots, n) \quad (32)$$

Introducing Eqs. 25 and 31 into Eq. 32, one obtains

$$\left(\frac{1}{m}\mathbf{K}_0^{-1}\Delta\mathbf{K} + \frac{1-m}{m}\mathbf{I}\right)\Phi_{k'}^* = \lambda_{k'}^*\Phi_{k'}^* \quad (33)$$

Rearranging Eq. 33

$$(\mathbf{K}_0^{-1}\Delta\mathbf{K})\Phi_{k'}^* = (m\lambda_{k'}^* - 1 + m)\Phi_{k'}^* \quad (34)$$

By comparing Eqs. 30 and 34, the following relationships are obtained:

$$\Phi_{k'}^* = \Phi_k \quad (35a)$$

$$\lambda_{k'}^* = \frac{(\lambda_k + 1 - m)}{m} \quad (35b)$$

If m is chosen in such a way that it satisfies the inequality $|\lambda_{k'}^*| < 1$ for all the k's, we obtain

$$|m| > |\lambda_k + 1 - m|, \qquad (k = 1, 2, \ldots, n) \quad (36)$$

Because of the positive definiteness of $\mathbf{K}$, all the λ_ks in Eq. 30 are larger than -1. If the largest positive eigenvalue is known as Max $[\lambda_k]$, we can select a range of m that satisfies Eq. 36 in the λ_k-m plane as

$$m > \frac{\text{Max}\,[\lambda_k] + 1}{2} \quad (37)$$

Then, such an m satisfies Eq. 36 for all the λ_ks. Therefore, the existence of an m that makes Neumann expansion possible is guaranteed, irrespective of how large the deviation $\Delta\mathbf{K}$ is.

Since the truncated Gaussian distribution is used later for Young's modulus variation in the numerical example, all the λs are always less than one. Thus, we need not introduce m in such cases. However, the foregoing discussion validates the Neumann expansion method for any possible variabilities in $\mathbf{K}$.

Perturbation Method

In order to demonstrate the difference between the Neumann expansion method and other existing techniques, a perturbation approximation involving terms up to the second order is described as a typical example of the analytical approach, primarily following Hisada and Nakagiri's (1981, 1985) notation.

If the stiffness matrix $\mathbf{K}$ involves a set of nondimensional random variables $\mathbf{a} = [a_1\ a_2\ \ldots\ a_n]^T$ which represents the material property variability, $\mathbf{K}$ can be expanded in the following form with the assumption that each a_i is small ($a_i \ll 1$) and has zero mean

$$\mathbf{K} = \mathbf{K}^0 + \sum_{i=1}^{n} \mathbf{K}_i^{\mathrm{I}} a_i + \frac{1}{2} \sum_{i=1}^{n} \sum_{j=1}^{n} \mathbf{K}_{ij}^{\mathrm{II}} a_i a_j + \cdots \quad (38)$$

in which $\mathbf{K}^0$ is the stiffness matrix evaluated at $\mathbf{a} = \mathbf{0}$, and $\mathbf{K}_i^{\mathrm{I}}$ and $\mathbf{K}_{ij}^{\mathrm{II}}$ are partial derivatives of $\mathbf{K}$ defined as follows:

$$\mathbf{K}_i^{\mathrm{I}} = \left.\frac{\partial \mathbf{K}}{\partial a_i}\right|_{\mathbf{a}=\mathbf{0}} \quad (39a)$$

$$\mathbf{K}_{ij}^{\mathrm{II}} = \left.\frac{\partial^2 \mathbf{K}}{\partial a_i \partial a_j}\right|_{\mathbf{a}=\mathbf{0}} \quad (39b)$$

If, although this is not the case considered herein, the external force vector $\mathbf{F}$ also involves random variables, $\mathbf{F}$ can be expanded in a form similar to that for $\mathbf{K}$. Assuming that the displacement vector $\mathbf{U}$ is also expanded as

$$\mathbf{U} = \mathbf{U}^0 + \sum_{i=1}^{n} \mathbf{U}_i^{\mathrm{I}} a_i + \frac{1}{2} \sum_{i=1}^{n} \sum_{j=1}^{n} \mathbf{U}_{ij}^{\mathrm{II}} a_i a_j + \cdots \quad (40)$$

its coefficient vectors, $\mathbf{U}^0$, $\mathbf{U}_i^{\mathrm{I}}$, and $\mathbf{U}_{ij}^{\mathrm{II}}$, are evaluated by the following set of recursive equations:

$$\mathbf{U}^0 = (\mathbf{K}^0)^{-1}\mathbf{F}^0 \quad (41)$$

$$\mathbf{U}_i^{\mathrm{I}} = (\mathbf{K}^0)^{-1}(\mathbf{F}_i^{\mathrm{I}} - \mathbf{K}_i^{\mathrm{I}}\mathbf{U}^0) \quad (42)$$

$$\mathbf{U}_{ij}^{\mathrm{II}} = (\mathbf{K}^0)^{-1}(\mathbf{F}_{ij}^{\mathrm{II}} - \mathbf{K}_i^{\mathrm{I}}\mathbf{U}_j^{\mathrm{I}} - \mathbf{K}_j^{\mathrm{I}}\mathbf{U}_i^{\mathrm{I}} - \mathbf{K}_{ij}^{\mathrm{II}}\mathbf{U}^0) \quad (43)$$

The strain $\boldsymbol{\varepsilon}_e$ and stress $\boldsymbol{\sigma}_e$ of element e are also expanded in similar series forms whose coefficients vectors can be determined properly.

The first-order approximation for the displacement is obtained by truncating the right-hand side of Eq. 40 after the second term as

$$\mathbf{U} = \mathbf{U}^0 + \sum_{i=1}^{n} \mathbf{U}_i^{\mathrm{I}} a_i \quad (44)$$

with expected value

$$E^{\mathrm{I}}[\mathbf{U}] = \mathbf{U}^0 \quad (45)$$

and covariance matrix

$$\mathrm{Cov}^{\mathrm{I}}[\mathbf{U}, \mathbf{U}] = E[(\mathbf{U} - E^{\mathrm{I}}[\mathbf{U}])(\mathbf{U} - E^{\mathrm{I}}[\mathbf{U}])^T] = \sum_{i=1}^{n} \sum_{j=1}^{n} \mathbf{U}_i^{\mathrm{I}} (\mathbf{U}_j^{\mathrm{I}})^T E[a_i a_j] \quad (46)$$

where $E[a_i\, a_j]$ is determined analytically from the autocorrelation function of the underlying stochastic field of a.

The second-order approximation for the displacement is also obtained by truncating the right-hand side of Eq. 40 after the third term as

$$\mathbf{U} = \mathbf{U}^0 + \sum_{i=1}^{n} \mathbf{U}_i^{\mathrm{I}} a_i + \frac{1}{2} \sum_{i=1}^{n} \sum_{j=1}^{n} \mathbf{U}_{ij}^{\mathrm{II}} a_i a_j \quad (47)$$

with expected value

$$E^{\mathrm{II}}[\mathbf{U}] = E^{\mathrm{I}}[\mathbf{U}] + \frac{1}{2} \sum_{i=1}^{n} \sum_{j=1}^{n} \mathbf{U}_{ij}^{\mathrm{II}} E[a_i a_j] \quad (48)$$

and covariance matrix

$$\mathrm{Cov}^{II}[\mathbf{U}, \mathbf{U}] = Cov^{I}[U, U]$$

$$+ \frac{1}{4} \sum_{i=1}^{n} \sum_{j=1}^{n} \sum_{k=1}^{n} \sum_{l=1}^{n} \mathbf{U}_{ij}^{\mathrm{II}} (\mathbf{U}_{kl}^{\mathrm{II}})^T (E[a_i a_l]E[a_j a_k] + E[a_i a_k]E[a_j a_l]) \quad (49)$$

In the process of deriving $\mathrm{Cov}^{\mathrm{II}}[\mathbf{U}, \mathbf{U}]$, the as are assumed to be Gaussian. If they are not Gaussian, one must evaluate their third- and fourth-order moments accordingly. The expected values and covariance matrices of the

strain and stress are also evaluated analytically in a manner similar to that for the displacement.

Numerical Example

Finite Element Model and Assumptions

A computer program was developed by which we could estimate the response variability due to material property variation. This program estimates the expected value and standard deviation of the response by means of Monte Carlo techniques. In doing so, two different Monte Carlo methods are used for the solution of Eq. 13: the direct method uses Eqs. 16 and 17 for each sample, while the Neumann expansion method uses an iterative scheme in the form of Eq. 22. A number of sample global stiffness matrices are constructed on the basis of the sample stochastic fields generated by means of Eq. 6. Then, the direct Monte Carlo simulation (direct M.C.S.) solution is obtained each time by employing one of the sample global stiffness matrices and taking statistics on the resulting response quantities. On the other hand, the simulation solution based on the Neumann expansion, referred to as the Neumann expansion Monte Carlo simulation or, for brevity, expansion Monte Carlo simulation (expansion M.C.S.), then uses Eq. 22 for Monte Carlo purposes. Another program based on the perturbation method, which involves first- and second-order perturbation approximations, is also developed. Numerical examples are presented here in order to examine the accuracy and efficiency of these methods.

The finite element model shown in Fig. 1 is adopted as an example. The particular structural geometry and loading conditions are chosen so that the response variability can be clearly highlighted by the material property variability. The model consists of 100 plane-stress square finite elements with 121 nodes. Nodal displacements in the y-direction are constrained along the lower edge, and nodal displacements in both directions are constrained at the left lower corner nodes. Under these boundary conditions, the number of degrees-of-freedom (DOF) of this structural system is 230. A uniformly distributed load is applied along the upper edge.

The median E_0 of Young's modulus is assumed to be $E_0 = 1.0$, while Poisson's ratio is assumed to be a constant, $\nu = 0.3$. In this example, all the parameters are represented without units so that any units can be specified so long as they are used consistently. The stochastic field $a(x)$ representing the deviatoric component of the material property is assumed to be isotropic with autocorrelation and spectral density functions as given in Eqs. 3 and 4, respectively. This stochastic field is discretized in accordance with the finite-element mesh shown in Fig. 1, and $a(\mathbf{x})$ in element e is represented by the value of a_e of $a(\mathbf{x})$ at the centroid $\mathbf{x}_e$ of the element as mentioned earlier; $a_e = a(\mathbf{x}_e)$ where the assumption that the variation of a within the element is small enough is used.

The autocorrelation function given by Eq. 3 includes two parameters, the standard deviation σ_0 and correlation distance d, and proper mesh division depends primarily on the values of these parameters because of the particular structural geometry and loading conditions considered. Three values of σ_0, i.e., 0.1, 0.2, and 0.3, and $d = 2.0$ are used throughout the numerical example.

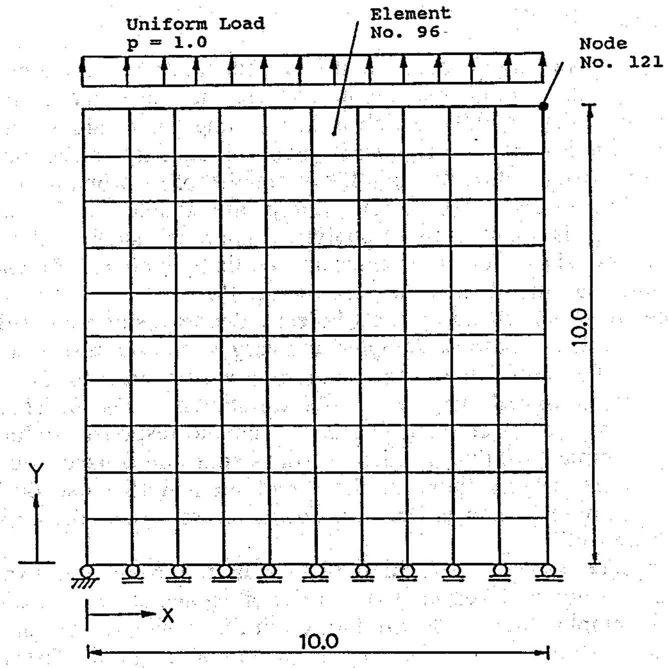

FIG. 1. Finite Element Model with 100 Elements

Our experience indicates that the element size in Fig. 1 is considered to be small enough in view of the fact that $d = 2.0$ in this case; the element size is one-half the scale of correlation (Harada and Shinozuka 1986a). The question of "in what sense is it small enough" is another matter to be studied. As mentioned in the introduction, however, the major concern of the present study is to examine the accuracy of the various analytical and numerical methods of variability prediction. Thus, once the stochastic field is discretized in the manner indicated, the accuracy problem can be dealt with as an issue separate from that of the mesh size.

The results of the numerical example will be shown at locations where large output values are expected, i.e., node 121 for displacement U_y and element 96 for strain ε_{yy}.

Example for Variation of E

Young's modulus is assumed to be Gaussian as indicated in the following:

$$E_e = E_0(1 + a_e) \qquad (50)$$

where E_e = the discretized version of $E(\mathbf{x})$ in element e; and a_e = a nondimensional random variable. In this case, the standard deviation of a_e represents the coefficient of variation of E_e. The assumption of Gaussian distribution implies the possibility of generating negative values of Young's modulus. In order to avoid this difficulty, the values of random variable a_e in the case of Monte Carlo simulation are confined to the range:

$$-1+\varepsilon \leqq a_e \leqq 1-\varepsilon \quad \ldots\ldots\ldots\ldots\ldots\ldots\ldots\ldots\ldots\ldots \quad (51)$$

in which ε = a positive constant that is introduced to avoid mathematical complications that would arise if a_e indeed becomes zero. In this numerical example, we use $\varepsilon = 0.05$, which is in the range of ε-values where the response statistics are not very sensitive to ε. Inequality on the right-hand side is also introduced to maintain the symmetry of its probability density function. The effect of these truncations are smaller if the standard deviation of a_e is smaller. In an analytical approach such as the perturbation method, these negative values are implicitly included if a Gaussian distribution is assumed as in the case of Eq. 49.

Samples of a_e simulated by the Cholesky decomposition algorithm are shown in Fig. 2. Using these samples, convergence of the response values obtained by the Neumann expansion method with respect to the order of expansion is examined. Typical results are shown in Fig. 3. This figure shows that the rate of convergence of the sample responses differs from sample to sample, and that, as higher order expansion is used, the results approach more closely those of the direct method (the use of Eq. 15 sample-by-sample, which is thus considered to represent the expansion order of infinity).

Convergence of the standard deviation in the Neumann expansion simulation method with respect to the order of expansion is also examined. Using 100 samples, the results are plotted in Fig. 4 with the results of the direct Monte Carlo simulation and perturbation method. The rate of convergence of the standard deviation is seen to be slower than that of the sample responses, although the results of the Neumann expansion simulation method eventually approach those of the direct Monte Carlo simulation method. This is partly due to the fact that the standard deviation plotted in Fig. 4 results from only the deviatoric component of the sample response, while the sample responses shown in Fig. 3 consist of mean values plus deviatoric components. It is also noted that the first- and second-order perturbation results are close to those of the first- and second-order Neumann expansion method, respectively. This implies that the accuracy of the perturbation method is comparable to the Neumann expansion simulation method of the same order, although no explicit convergence criterion exists for the perturbation method.

In the case of Monte Carlo simulation, we must examine whether or not the sample size is large enough to represent the exact solution. The statistical fluctuation of the standard deviation evaluated by means of direct Monte Carlo simulation is shown in Fig. 5 as a function of the sample size (triangles connected by dashed lines). Observing Fig. 5, we decided to use a sample size equal to 100 for the following reasons: (1) While the fluctuation is observed after 100 samples, it falls within a tolerable range (between 0.38–0.46); (2) Fig. 5 represents the worst case, corresponding to a coefficient of variation V_E of Young's modulus equal to 0.3 (this value of V_E applies to Gaussian distribution before truncation) (for smaller values of the coefficient of variation, statistical stability is much better); and, most importantly, (3) with a sample size of 100, we can well demonstrate the difference in trend in which the standard deviation increases as V_E also increases. The expected value of ε_{yy} estimated by the direct Monte Carlo simulation method indicates (Yamazaki et al. 1985) that a satisfactory

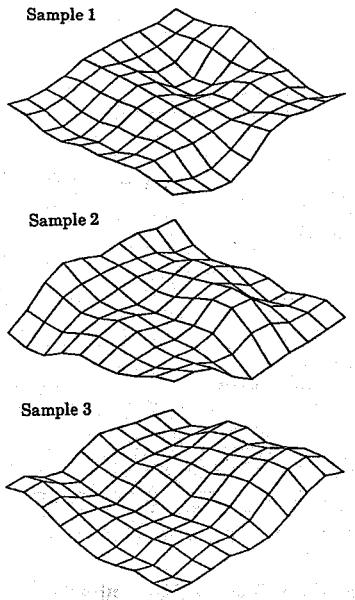

FIG. 2. Simulated Sample Variations of Young's Modulus

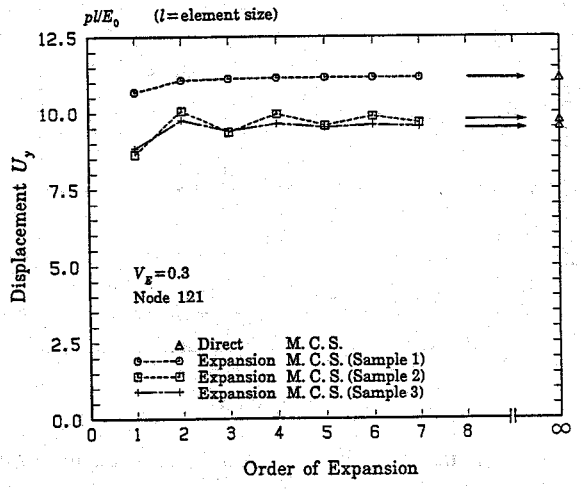

FIG. 3. Convergence of Displacement U_y (Variation of E)

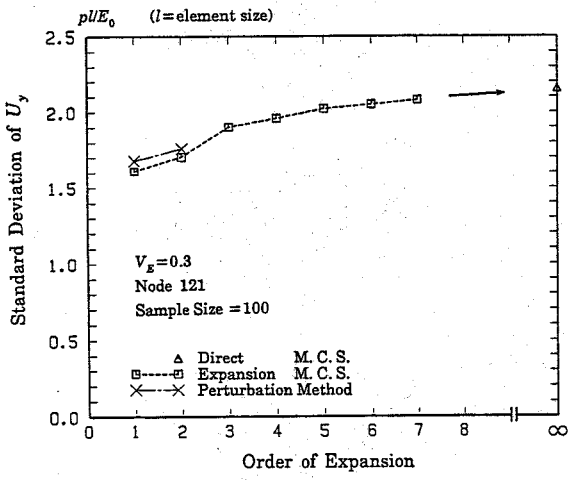

FIG. 4. Convergence of Standard Deviation of U_y (Variation of E)

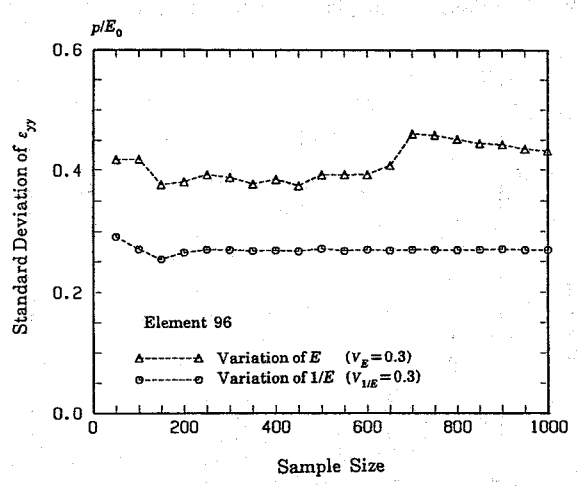

FIG. 5. Standard Deviation of ε_{yy} by Direct M.C.S. as Function of Sample Size

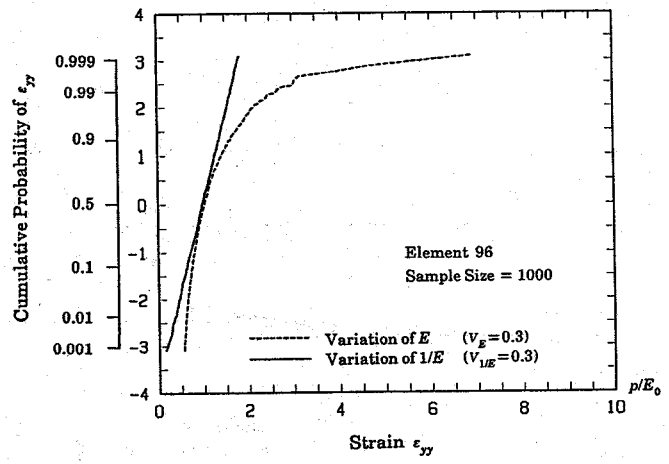

FIG. 6. Statistical Distribution of ε_{yy} by Direct M.C.S. Plotted on Gaussian Probability Paper

stability can be obtained with even a smaller sample size and a much smaller fluctuation. In passing, it is mentioned that Fig. 5 also plots the standard deviation of ε_{yy} where $1/E$ rather than E is Gaussian (circles connected by dashed lines), and that in this case, statistical stability is achieved much more rapidly and smoothly than in the case where E is Gaussian. Actually, when E is Gaussian with a coefficient of variation V_E as large as 0.3, the statistical distribution of ε_{yy} becomes highly skewed as shown in Fig. 6 (dashed lines). This is due to the fact that the element stiffness can approach a very small value with a relatively large probability since V_E is as large as 0.3. On the other hand, the corresponding distribution function in the case of $1/E$ being Gaussian is close to Gaussian, as shown in Fig. 6 (solid line).

The direct and expansion M.C.S. analyses and first-order and second-order perturbation analyses are performed for three values of V_E. Second-order perturbation analysis can be performed for only one element at a time because of the enormous CPU time and huge memory space the analysis requires.

The results of the computation by these four methods (direct M.C.S., expansion M.C.S., and first- and second-order perturbation) are shown in Figs. 7 and 8 as a function of V_E, Fig. 7 for the expected value, and Fig. 8 for the standard deviation of ε_{yy}. It is noted that in the range of small values of V_E, the results of all these methods are very close.

In Fig. 7, a moderate increase is observed for the expected value of ε_{yy} and V_E increases. This observation applies to whichever of the four methods is used, except for the first-order perturbation method, in which case the expected value remains constant regardless of the value of V_E. In Fig. 8, the standard deviation of ε_{yy} is shown to increase linearly when estimated by the first-order perturbation method. This represents a considerable underestimation of the standard deviation, which can be only slightly improved by the implementation of a second-order perturbation approximation as also shown in Fig. 8. This result obtained from the

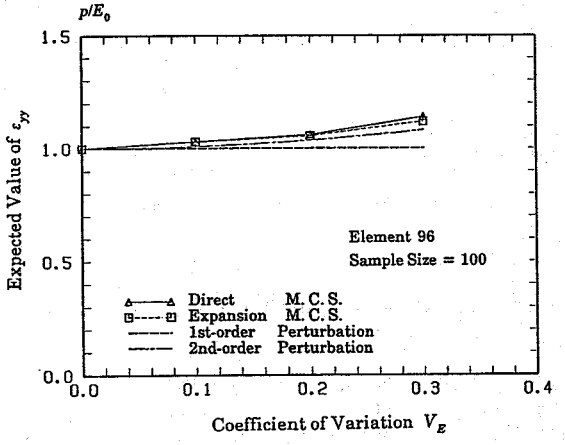

FIG. 7. Comparison of Expected Value of ε_{yy} (Variation of E)

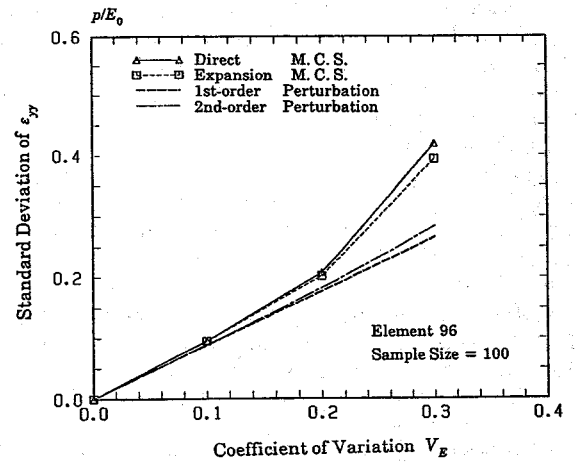

FIG. 8. Comparison of Standard Deviation of ε_{yy} (Variation of E)

TABLE 1. Comparison of CPU Time (230 DOF Model)

Monte Carlo Simulation (Sample Size = 100)		Perturbation Method	
Direct method (1)	Neumann expansion method (2)	First-order approximation (3)	Second-order approximation (4)
00:15:05[a]	00:09:01 (first) 00:10:10 (second) 00:11:19 (third)	00:03:58	04:46:09 (for one element)

[a]Hour:minute:second.

second-order perturbation approximation is disappointing, particularly because it requires an enormous amount of computational time as well as memory space. In contrast to the results provided by the perturbation methods, the standard deviation estimated by the Monte Carlo methods is shown in Fig. 8 to have an accelerated rate of increase as V_E increases. The estimated standard deviation by the expansion M.C.S. method is close to that of the direct M.C.S. method.

It may be observed in Fig. 8 that perturbation methods, whether first- or second-order, underestimate the response variability for large values of V_E, for which such a response variability analysis is particularly significant. It is important to note that this result is consistent with earlier results as demonstrated, for example, in Shinozuka and Astill (1972), Shinozuka and Wen (1972), and Vaicaitis et al. (1973).

Referring to the CPU time, Table 1 compares the CPU time on a VAX 11/750 in estimating the expected value and standard deviation for all the response quantities (displacement vector as well as stress and strain tensors). The direct M.C.S. method requires more time than does the expansion M.C.S. method. How much more, however, depends on many factors, including the order of expansion, variability of input (V_E), desired level of accuracy (Eq. 23), number of DOF in the system, and the band-width of the stiffness matrix. In the present example, the use of Eq. 23 requires third-order expansion for the expansion M.C.S. method in the case where $V_E = 0.3$ on the average. On the basis of counting the number of units of add-multiply operations involved in the algorithm mentioned earlier, it can be shown that, if the order of Neumann expansion is fixed and not too large, the expansion method will be more advantageous in terms of CPU time as the number of DOF increases. For example, the ratio of CPU time required for the expansion M.C.S. method to that for the direct M.C.S. method is of the order of 1/50, when the sample size = 100, the order of expansion = 3, the number of DOF = 10,000, and the band-width = 1,000 ~ 2,500.

Table 1 also indicates that the first-order perturbation method requires the least amount of CPU time, as expected. However, second-order perturbation approximation, even for only one element, requires by far the greatest amount of CPU time, suggesting that this approximation method is quite impractical.

A very similar response variability as shown here was obtained in Yanazaki et al. (1987), in which E is considered to form a stochastic field

having a beta distribution as a one-dimensional distribution instead of a truncated Gaussian distribution. The response variability when $1/E$, $\log E$, or ν is considered to form a Gaussian field is also estimated by Yamazaki et al. (1985). In these cases, however, agreement among the response variabilities estimated by the four methods mentioned is much better than the case in which E itself is a stochastic field. In fact, the agreement is good even when the coefficient of variation of $1/E$, $\log E$, or ν is relatively large. Therefore, for the Gaussian or truncated Gaussian variability of $1/E$, $\log E$, or ν, the first-order perturbation method is found to be quite efficient. The reader is reminded that the strain ε_{yy} has a Gaussian distribution in approximation when $1/E$ is a Gaussian field (see Fig. 6). It can also be demonstrated that the same is true when $\log E$ or ν is a Gaussian field. This is the reason that the first-order perturbation method works fairly well under these conditions. Even in these cases, however, it is necessary to perform a direct or expansion M.C.S. at least once for each problem in order to verify the accuracy of the perturbation analysis.

Conclusions

A Neumann expansion method has been developed and used for evaluating the effect of spatially varying material properties within the framework of linear static structural analysis, and in conjunction with Monte Carlo simulation methods. The advantages of the proposed method are summarized as follows:

1. CPU time is reduced in comparison with the direct M.C.S. method by using the result of the stiffness matrix factorization, which is performed only once for the entire sample of structures.
2. The convergence of the series solution is guaranteed for each sample structure and can be confirmed numerically and graphically.
3. Existing deterministic finite element analysis programs can be easily used.

A first- and second-order approximation analysis program based on the perturbation technique was also developed. Numerical examples revealed the following features of the perturbation technique in comparison with the simulation methods:

1. The first-order perturbation analysis shows good agreement with Monte Carlo simulation results in the range of small variability of the elastic modulus, while requiring a much smaller amount of CPU time than the expansion M.C.S.
2. The first-order analysis does not agree with the simulation results in the range of large variability of Young's modulus if the Young's modulus is assumed to be truncated Gaussian.
3. A second-order perturbation analysis can improve the results of the first-order analysis only a little. However, second-order analysis requires an enormous amount of CPU time, much more than the direct M.C.S. solution does.
4. A first-order analysis may be quite useful depending on the type of stochastic fields to which the material property in question subscribes. However, the results should be verified by Monte Carlo simulation techniques.

Acknowledgments

This work was supported by the National Science Foundation under Grant No. ECE-85-15249 with Dr. S-C. Liu as Program Director. Also, grateful acknowledgement is made to the Shimizu Construction Co., Ltd., of Tokyo, Japan, for its financial support of the first writer during his stay at Columbia University.

Appendix. References

Astill, C. J., Nosseir, B., and Shinozuka, M. (1972). "Impact loading on structures with random properties." *J. Struct. Mech.*, 1(1), 63–77.
Baecher, G. B., and Ingra, T. S. (1981). "Stochastic FEM in settlement predictions." *J. Geotech. Engrg. Div.*, ASCE, 107(GT4), 449–463.
Cambou, B. (1975). "Application of first-order uncertainty analysis in the finite element method in linear elasticity." *Proc., 2nd Int. Conf. on Applications of Statistics and Probability in Soil and Struct. Engrg.*, 67–87.
Der Kiureghian, A. (1985). "Finite element methods in structural safety studies." *Proc. Structural Safety Studies Symposium*, in conjunction with the ASCE Convention in Denver, Colo., 40–52.
Handa, K., and Andersson, K. (1981). "Application of finite element methods in the statistical analysis of structures." *Proc. 3rd ICOSSAR*, 409–417.
Harada, T., and Shinozuka, M. (1986b). *The scale of correlation for stochastic fields—technical report.* Department of Civil Engineering and Engineering Mechanics, Columbia University, New York, N.Y.
Harada, T., and Shinozuka, M. (1986a). "Ground deformation spectra." *Proc. 3rd U.S. Nat. Conf. on Earthquake Engineering*, Charleston, S.C., 2191–2202.
Hisada, T., and Nakagiri, S. (1981). "Stochastic finite element method developed for structural safety and reliability." *Proceedings of the 3rd ICOSSAR*, June 1981, pp. 395–408.
Hisada, T., and Nakagiri, S. (1985). "Role of the stochastic finite element method in structural safety and reliability." *Proc. 4th ICOSSAR*, 385–394.
Inference Corporation. (1983). "SMP—a symbolic manipulation program." *Reference Manual, Version 1*, Inference Corp., Los Angeles, Calif.
Iyengar, R. N., and Shinozuka, M. (1972). "Effect of self-weight and vertical acceleration on the behavior of tall structures during earthquake." *J. Earthquake Engrg. Struct. Dyn.*, 1, 69–78.
Lumley, J. L. (1970). *Stochastic tools in turbulence.* Academic Press, New York, N.Y.
Monin, A. S., and Yaglom, A. M. (1971). *Statistical fluid mechanics: mechanics of turbulence*, J. L. Lumley, ed., MIT Press, Cambridge, Mass.
Naganuma, T., Deodatis, G., and Shinozuka, M. (1987). "ARMA Model for Two-Dimensional Processes," *J. Engrg. Mech.*, ASCE, 113(2), 234–251.
Shinozuka, M. (1972a). "Probabilistic modeling of concrete structures." *J. Engrg. Mech. Div.*, ASCE, 98(EM6), 1433–1451.
Shinozuka, M. (1927b). "Monte Carlo simulation of structural dynamics." *Int. J. Comput. Struct.*, 2, 855–874.
Shinozuka, M. (1974). "Digital simulation of random processes in engineering mechanics with the aid of the FFT technique." *Stochastic problems in mechanics*, S. T. Ariaratnam and H. H. E. Leipholz, eds., University of Waterloo Press, Waterloo, Canada, 277–286.
Shinozuka, M. (1987). "Stochastic fields and their digital simulation." *Stochastic Methods in Structural Dynamics*, G. I. Schuëller and M. Shinozuka, eds., Nijhoff Publishers, Netherlands, 93–133.
Shinozuka, M., and Astill, C. J. (1972). "Random eigenvalue problems in structural

mechanics." *AIAA J.*, 10(4), 456–462.
Shinozuka, M., and Deodatis, G. (1988). "Response Variability of Stochastic Finite Element Systems." *J. Engrg. Mech.*, ASCE, 114(3), 499–519.
Shinozuka, M., and Jan, C-M. (1972). "Digital simulation of random processes and its applications." *J. Sound Vib.*, 25(1), 111–128.
Shinozuka, M., Vaicaitis, R., and Asada, H. (1976). "Digital simulation of random forces or large-scale experiments." *AIAA J.*, 13(6), 425–431.
Shinozuka, M., and Wen, Y-K. (1972). "Monte Carlo solution of nonlinear vibrations." *AIAA J.*, 10(1), 37–40.
Shinozuka, M., Yun, C-B., and Vaicaitis, R. (1977). "Dynamic analysis of fixed offshore structures subjected to wind-generated waves." *J. Struct. Mech.*, 5(2), 135–146.
Tatarski, V. I. (1961). *Wave propagation in a turbulent medium*. McGraw–Hill, New York, N.Y.
Vaicaitis, R., Jan, C-M., and Shinozuka, M. (1972). "Nonlinear panel response and noise transmission from a turbulent boundary layer by a Monte Carlo approach." *AIAA J.*, 10(7), 895–899.
Vaicaitis, R., Shinozuka, M., and Takeno, M. (1973). "Parametric study of wind loading on structures." *J. Struct. Div.*, ASCE, 99(ST3), 453–468.
Vanmarcke, E. (1983). *Random fields*. MIT Press, Cambridge, Mass.
Vanmarcke, E., and Grigoriu, M. (1983). "Stochastic finite element analysis of simple beams." *J. Engrg. Mech.*, ASCE, 109(5), 1203–1214.
Yamazaki, F., Shinozuka, M., and Dasgupta, G. (1987). "Addendum to 'Neumann expansion for stochastic finite element analysis.'" In *Stochastic Mechanics*, Vol. I, Columbia University, New York, N.Y., 245–251.
Yamazaki, F., Shinozuka, M., and Dasgupta, G. (1985). *Neumann expansion for stochastic finite element analysis—technical report*. Department of Civil Engineering and Engineering Mechanics, Columbia University, New York, N.Y.